Journal of Bioscience and Bioengineering
VOL. 128 No. 1, 88–97, 2019

www.elsevier.com/locate/jbiosc

Date pits activated carbon for divalent lead ions removal

Rambabu Krishnamoorthy,[1,2] Bharath Govindan,[2] Fawzi Banat,[2] Velu Sagadevan,[1]
Monash Purushothaman,[1] and Pau Loke Show[3,*]

Department of Chemical Engineering, School of Civil and Chemical Engineering, VIT University, Katpadi Road, Vellore 632014, India,[1] *Department of Chemical Engineering, Khalifa University of Science and Technology, The Petroleum Institute, Al Saada Street, Abu Dhabi 127788, United Arab Emirates,*[2] *and Department of Chemical Engineering, The University of Nottingham-Malaysia Campus, Jalan Broga, 43500 Selangor Darul Ehsan, Malaysia*[3]

Received 4 October 2018; accepted 17 December 2018
Available online 22 January 2019

Phosphoric acid impregnated activated carbon from date pits (DPAC) was prepared through single step activation. Prepared DPAC was studied for its structural, elemental, chemical, surface and crystal nature. Adsorption ability of the DPAC was assessed through divalent lead ions separation studies. Effect of adsorbent dosage, contact time, pH, operating temperature and initial feed concentration on lead removal by DPAC was studied. Maximum Pb(II) adsorption capacity of 101.35 mg/g was attained for a contact time of 30 min and pH of 6 at 30°C. Increase in initial feed concentration enhanced the adsorption ability of DPAC and the rise in adsorbent dosage resulted in improved Pb(II) removal efficiency. Thermodynamic studies revealed that the lead adsorption on DPAC was exothermic and instantaneous in nature. Kinetic and equilibrium studies confirmed the suitability of pseudo-second order and Langmuir isotherm for divalent lead ions binding on DPAC. Reusability studies showed that HCl was the effective regeneration medium and the DPAC could be reused for a maximum of 4 times with slight reduction in Pb(II) removal efficiency (<10%). Results indicated the promising use of date pits biomass as a low cost and efficient starting material to prepare activated carbon for divalent lead ions removal.

[**Key words:** Activated carbon; Date pits; Lead ions; Chemical activation; Adsorption]

Separation of toxic metal ions from the drinking water and industrial aqueous streams is a highly explored research field (1). Lead ion is one such toxic contaminant present in nature and industrial wastewaters, usually in the divalent form (2). Wastewaters discharged by electroplating, dye and paint, battery manufacture, glass industries and so on contain a high level of lead ions which needs effective separation before discharge (3). Accumulation of these non-degradable lead ions over time in aqueous streams causes severe ecological and environmental problems (4). Consumption of lead contaminated water can cause anemia, brain damage, cancer and even fatality in case of humans (4,5). Impotency, miscarriage and stillbirth are also attributed to lead poisoning effects in humans (6). World Health Organization norms restrict the level of lead ions to 0.01 ppm in drinking water (7,8). Hence complete elimination of lead ions from the aqueous streams is a very essential step in the domestic water as well as industrial wastewater treatment process.

Various physio-chemical processes namely chemical precipitation, electro-chemical precipitation, electro-dialysis, adsorption, ion exchange and membrane technology are commercially available for the separation of lead ions from the wastewater streams (8). Recently, solid phase extraction of analytes using different types of sorbents including metallic nanoparticles is being explored (9–16). However, use of excessive chemicals, generation of toxic sludge, need of additional separation steps and high cost are the major disadvantages associated with these processes. Adsorption is still one of the preferred separation processes due to its economic feasibility and technical ease (17). Adsorption technique is highly preferred for removal of elements present in trace levels in aqueous streams (18). Activated carbon used as a predominant adsorbent in the adsorption process is a carbonaceous substance known for its high porosity, large specific surface area and better mechanical strength (19). As compared to biosorbents, activated carbon possess better adsorption capacity, high surface area, better stability, excellent thermal resistance and inertness to adsorption conditions making them as an ideal choice (20). Removal of various toxic pollutants including metals, dyes, and gases by activated carbon has made the activated carbon based adsorption system very attractive, especially for lead removal from its aqueous streams (20,21).

High cost and less reusability of commercial activated carbon has led to development of waste biomasses derived activated carbon, having better adsorption capacities (22). These biomasses mainly consist of agricultural wastes having a rich content of cellulose, hemicelluloses and lignin components (23). Various agricultural biomasses such as papaya peel (24), sugarcane bagasse (25), oak shell (26), pinecone (27), hazelnut husks (28), coconut shells (29), cow bone (30) have been studied for activated carbon preparation and their application for lead ions separation. Carbon derived from the biomasses could be activated by either physical or chemical means. Physical activation is a two-step process, (i)

---

[*] Corresponding author at: Department of Chemical Engineering, The University of Nottingham-Malaysia Campus, Jalan Broga, 43500 Selangor Darul Ehsan, Malaysia. Tel.: +60 10 225 0322; fax: +60 3 8924 8020.

E-mail addresses: showpauloke@gmail.com, Pauloke.show@nottingham.edu.my (P.L. Show).

1389-1723/$ – see front matter © 2019, The Society for Biotechnology, Japan. All rights reserved.
https://doi.org/10.1016/j.jbiosc.2018.12.011

carbonization step which produces non-porous char and (ii) activation step using carbon dioxide (CO_2) or steam, to enhance the textural properties (31). Chemical activation involves simultaneous carbonization and activation using chemical reagents such as zinc chloride ($ZnCl_2$), sulphuric acid (H_2SO_4), phosphoric acid (H_3PO_4), potassium hydroxide (KOH) and sodium hydroxide (NaOH) as the activating agents (32). Acid based activation incorporates a large amount of −COO groups on the carbon surface in addition to increase in surface areas. These negatively charged carboxylic groups provide additional activity for adsorbate removal especially for heavy metals like lead, cadmium, cobalt, and mercury.

Low ash content, well defined natural structure and enhanced lignocellulosic composition make dates pits as suitable starting materials for production of activated carbon (33). However, limited literature and research works have been carried out with the date seeds for activated carbon synthesis (34). High porosity activated carbon through pyrolysis and physical activation using steam was developed from date seeds (35). Physiochemical activated carbon derived from date pits using CO_2 and KOH as activating mediums was studied for bentazon and carbofuran removal (36). Hydrothermal carbonized and NaOH activated carbon derived from date seed was employed for methylene blue dye separation studies (37). Date pits activated carbon using $ZnCl_2$ was effectively used to remove metallic salts and reduce BOD for textile and tannery effluents (38).

For the reported work, date pits activated carbon (DPAC) using H_3PO_4 as the activating agent was synthesized from date pits using single step approach. The obtained activated carbon was characterized for its structure, porosity parameters and functional groups. Prepared activated carbon was used to study its divalent lead (Pb(II)) adsorption ability in batch mode. Different adsorption factors namely initial feed concentration, operational temperature, adsorbent dosage, contact time and pH were studied to understand their effects on Pb(II) separation by DPAC. Thermodynamic analysis was performed to examine the Pb(II) adsorption nature on DPAC surface. Adsorbate-adsorbent interactions based various sorption isotherms were tested for equilibrium binding of Pb(II) molecules on DPAC surface. Time based adsorption data were correlated and studied with standard kinetic models. The reusability of the DPAC for Pb(II) removal was also analyzed using different regeneration mediums. The obtained experimental observations and results are discussed. The main novelty of this investigation is to highlight the usage of waste date pits biomass as a potential sorbent for the removal of toxic divalent lead ions from its aqueous solution. Also the phosphoric acid activated date pits was prepared through one-pot approach as compared to the conventional chemical activation which involves two different heat treatment steps for carbonization and activation.

MATERIALS AND METHODS

Materials Date pits were collected from the date fruits (Kimia variety) purchased at the local market. These seeds were thoroughly washed in distilled water for 3 times and sun dried thoroughly. Subsequently, the pits were powdered in a high speed rotary mill and sieved through mesh no. 100 (ASTM−E11). The collected date pit powder was preserved in a tight enclosure for further usage. Analytic grade chemicals and solutions procured from Merck, India were employed in this study. Fresh distilled water was used for all solutions preparation and wash purposes.

Preparation of activated carbon The seed powder was washed thoroughly and dried at 120°C for 8 h. Subsequently, the powder was soaked with phosphoric acid (85% H_3PO_4) for a weight (seed powder) by volume (acid) ratio of 1:2.5. After 12 h of impregnation, the filtered date pits powder was subjected to carbonization in a muffle furnace maintained under continuous nitrogen flow. The carbonization was carried out at 650°C for 120 min. The cooled carbon samples were removed from the furnace and washed repeatedly till neutral pH. DPAC were then dried and preserved at room temperature in air-tight closed bottles.

Characterization of activated carbon Brunauer-Emmett-Teller (BET) method was applied for the determination of specific surface area (S_{BET}). Total pore volume was estimated by the volume of nitrogen gas adsorbed (at a relative pressure of 0.98) to the DPAC surface per unit mass of the sample taken. Fourier transform infrared spectroscopy (FTIR), X-ray photoelectron spectroscopy (XPS) and Boehm's titration were carried out to understand the surface chemistry of the DPAC powder. FTIR analysis was performed on the DPAC in an IR spectrophotometer (IR Affinity−1, Shimadzu, Kyoto, Japan) with KBr pellet over the range of 4000 to 400 cm^{-1}. Spectral resolution was 2 cm^{-1} and the obtained spectra were corrected for the KBr background. The XPS spectra of the fresh DPAC was obtained on an XPS spectroscope (AXIS Nova, Manchester, UK) with pass energy of 20 eV. The quantity of various surface functional groups on the prepared activated carbon was estimated through Boehm's method using the standard reagents (27).

Structural and elemental properties of the synthesized DPAC were analyzed through X-ray diffraction (XRD), scanning electron microscopy (SEM) and energy dispersive X-ray analysis (EDX) studies. Crystalline nature of the fresh and spent DPAC samples was analyzed in an XRD instrument (Bruker D8 Advance, Bruker, UK) at step intervals of 0.02. SEM equipment (Evo-18, Carl Zeiss, USA) was used to understand the pore structure of the DPAC samples. EDX was carried out to determine the elemental composition of DPAC powder samples. SEM and EDX studies were performed for both fresh and Pb(II) loaded DPAC samples.

Batch adsorption studies Various sample feed solutions required for the Pb(II) adsorption studies were obtained from a feed stock $Pb(NO_3)_2$ solution of 1000 ppm. The pH of the prepared feed samples for adsorption studies was adjusted by buffer solutions. Lead ions adsorption studies on the prepared DPAC were carried out in batch mode. The feed solution was introduced into the flasks containing a definite amount of the DPAC adsorbate, at a specified initial concentration and operating temperature. Following parameters were studied in their specified range to understand their effects towards Pb(II) adsorption on the DPAC surface: contact time for 1−120 min, pH for 2−7, operating temperature for 30−60°C, adsorbent dosage for 0.5−4 g/L (DPAC powder in unit litre of $Pb(NO_3)_2$ solution) and feed solution concentration for 5−50 mg/L. The choice of the parameters and their value ranges were identified by thorough literature survey and related works for Pb(II) ions removal by adsorption. Adsorption tests were carried out under thorough mixing using a magnetic stirrer at an agitation speed of 300 rpm. Reported values are average of the experiments carried out in triplicate. Adsorption batch run was performed using 50 mL volume feed solution having an initial concentration of 50 mg/L treated with 0.1 g of adsorbent at pH 6 and contact time of 30 min at 30°C, unless otherwise specified.

Test samples were collected at prescribed intervals and subjected to centrifugation for five minutes at 3000 rpm. Pb(II) concentration in the supernatant was estimated through an atomic absorption spectrophotometer (ZA3000, Hitachi, Tokyo, Japan). Divalent lead removal percentage (%R) was estimated by the formula:

$$\%R = \frac{C_i - C_e}{C_i} \times 100 \tag{1}$$

where C_i and C_e are the Pb(II) concentrations (mg/L) pertaining to initial and equilibrium states of adsorption.

Pb(II) adsorption capacity after time t (min) of adsorption for the DPAC (q_t) was calculated using the formula,

$$q_t = \frac{(C_i - C_t) \times V_f}{W_a} \tag{2}$$

where C_t (mg/L), V_f (L) and W_a (g) are concentration of Pb(II) after time t, volume of feed solution taken and the weight of the DPAC adsorbent used. Equilibrium adsorption capacity (q_e) for the prepared DPAC was calculated from Eq. 2 using C_e instead of C_t.

Reusability studies Investigations were performed to regenerate the lead ions loaded DPAC and their successive reuse as adsorbent for Pb(II) removal. Reusability of the DPAC adsorbent is very important as it decides the economic success for synthesized activated carbon and lowers the spent adsorbent level (30). Three different regeneration mediums, distilled water, 0.01 M hydrochloric acid and 0.01 M sodium hydroxide, were tested for their effective desorption of divalent lead ions from the used-up DPAC adsorbent. Fixed quantity of Pb(II) adsorbed DPAC powder was introduced to 50 mL of the desorption solvent in Erlenmeyer flask and the solution mixture was stirred at a constant speed of 300 rpm using magnetic stirrer. Regenerated DPAC absorbent was then filtered, washed, dried and used for further adsorption studies.

Equilibrium isotherm studies Isotherm models of Langmuir, Freundlich and Temkin were matched with experimental equilibrium values. According to Langmuir theory, absence of molecular interactions between adsorbate results in single layer deposition on the adsorbent surface. The adsorbent possesses identical active sites and has a restricted adsorption capacity (q_{max}). According to Langmuir, the relation between C_e and q_e in a linearized form is presented as (39)

$$\frac{C_e}{q_e} = \frac{1}{q_{max} \times K_L} + \frac{C_e}{q_{max}} \tag{3}$$

where q_{max} (mg/g) and K_L (L/mg) are the monolayer maximum adsorption capacity and the adsorption constant for Langmuir isotherm, respectively. Separation factor (R_L) explicates the favor of adsorption if $0 < R_L < 1$ and is given by the expression (29):

$$R_L = \frac{1}{1+K_L C_i} \tag{4}$$

Freundlich isotherm assumes interactions among adsorbed molecules resulting in multi-layer formation on the adsorbent surface (40). Freundlich isotherm relates C_e and q_e linearly as:

$$\ln(q_e) = \ln\left(K_f\right) + \frac{1}{n} * \ln(C_e) \tag{5}$$

where K_f ($mg^{1-1/n}$ $L^{1/n}$/g) and n are the adsorption constant for Freundlich isotherm and the adsorption intensity, respectively.

Temkin isotherm postulates the theory of indirect adsorbate/adsorbate interactions resulting in decreased heat of adsorption (41). The linear relation between ln (C_e) and q_e is given by the equation:

$$q_e = \frac{RT}{b}\ln(K_t) + \frac{RT}{b}\ln(C_e) \tag{6}$$

where K_t (L/mg) is Temkin isotherm constant, b (J g/mol mg) is adsorption energy variation factor, R (J/mol K) is universal gas constant and T (K) is absolute temperature.

Kinetic studies Adsorption dynamics experiments for lead ions binding on the DPAC powder were carried out. The obtained experimental data were then fitted with the described kinetic models to understand the adsorption dynamics pattern. Pseudo-first order model relates q_t linearly with time (t) as (24)

$$\ln(q_e - q_t) = \ln(q_e) - k_1 * t \tag{7}$$

where k_1 is the pseudo-first order rate constant (1/min).

The linear relational form between q_t and t according to pseudo-second order kinetic model is given as (25)

$$\frac{t}{q_t} = \frac{1}{k_2 \times q_e^2} + \frac{t}{q_e} \tag{8}$$

where k_2 is the pseudo-second order rate constant (mg/g min).

Elovich kinetic model is more suited for chemisorption process relating q_t and t in a linear fashion as shown below (14):

$$q_t = \frac{1}{\beta_E}\ln\left(\frac{\alpha_E}{\beta_E}\right) + \frac{1}{\beta_E}\ln(t) \tag{9}$$

where α_E (mg/g min) and β_E (g/mg) are the initial adsorption rate and the desorption constant, respectively.

RESULTS AND DISCUSSION

Performance of various adsorbents for Pb(II) adsorption Pb(II) adsorption tests were carried out using various adsorbents derived from date pits and the adsorption capacity of the adsorbents is presented in Table 1. The various adsorbents are: (i) raw date pit powder (RDPP), (ii) dried date pit powder at 100°C for 24 h ($DP_{100,24}$) , (iii) phosphoric acid impregnated date pit activated carbon (DPAC), (iv) potassium hydroxide impregnated activated carbon (KOH-DPAC) which was synthesized by the same procedure of DPAC preparation except for the usage of potassium hydroxide as the activation agent instead of phosphoric acid and (v) commercial activated carbon (commercial AC). As presented in Table 1, DPAC possessed the highest lead ions binding ability while raw date pit powder recorded the lowest performance. DPAC produced 1.8 times better adsorption of lead ions as compared to commercial AC under similar adsorption conditions. Also, it was observed that the DPAC had a adsorption ability of two times more as compared with the alkali based date pit activated carbon (KOH-DPAC). Hence the acid based activated carbon derived from date pits powder was selected for further studies to investigate the impact of adsorption parameters on Pb(II) elimination from its aqueous solution.

TABLE 1. Performance of various date pits adsorbents for adsorbent dosage of 0.05 g.

Adsorbent	Pb(II) adsorption capacity (mg/g)
Raw date pits powder (RDPP)	10.53
$DP_{100,24}$	31.69
KOH-DPAC	55.27
DPAC	115.83
Commercial AC	64.18

Characterization of DPAC adsorbent Surface area analysis for the raw date pit powder and the DPAC were performed by N_2 adsorption/desorption studies. Table 2 contains the results for the textural parameters studies. Increase in the surface area and average pore radius for DPAC as compared to raw date pit powder clearly indicated the pore structure promotions due to phosphoric acid activation. Larger pore radius of DPAC could promote the particle diffusion within the adsorbent and thus increase the adsorption capacity (42).

XPS is an ideal method for investigating the surface composition and oxidation state information of the activated carbon which were prepared from date pits. Fig. 1 shows the wide spectra obtained for the fresh DPAC sample which exhibit two intense peaks at 286 and 530 eV corresponding to carbon (C 1s) and oxygen (O 1s), respectively. Insets of Fig. 1 show the deconvolution spectrum of the carbon and oxygen molecules pertaining to 1s status. Deconvolution of the C 1s spectra consists of three component peaks. In particular, the spectra at 285.5 eV can be assigned to sp^2 hybridized carbon (C=C). Weak intense peaks in the range of 289.4 and 290.1 eV indicate the presence of carbonyl/carboxylic groups and π-π* shake up satellite peak, respectively (31). In the case of O 1s, three types of O-containing groups could be verified on the surface of the prepared carbons, including the functional groups of C–O, C=O, and O–C=O corresponding to peaks at 531.4, 531.8, and 534.7 eV, respectively (22).

Boehm titration results for the concentration of different surface functional groups of raw date pit powder and DPAC are presented in Table 2. Results showed that there was a balance of total acidic and basic functional groups in DPAC. Concentration sequence for the acidic functional groups was: carboxyl > phenolic > lactone. The increased acidic group concentration on DPAC surface, especially the carboxyl amount, presents a good potential for metal ion adsorption to its surface. The reduction in the basic functional group for DPAC as compared to raw date pit powder is ascribed to the phosphoric acid activation (43).

Phase purity, chemical and structural natures for the pristine and spent DPAC was investigated by XRD, FTIR and SEM techniques. Fig. 2A illustrates the XRD patterns for fresh and lead loaded DPAC. The broad diffraction peak seen at 2θ = 22° represents the graphite crystallinity in both samples. The absence of any characteristic peak in the fresh DPAC clearly indicated the amorphous nature of the adsorbent. This amorphous nature of the adsorbent aids for the easy diffusion of Pb(II) ions to its surface and would cause an effective lead ions removal (44). In case of the spent DPAC, a mild shift of the broad amorphous peak was observed which was due to

TABLE 2. Textural parameters and surface chemistry for the raw date pits and DPAC surfaces.

Sample	BET specific surface area, S_{BET} (m^2/g)	Average pore radius, R_m (nm)	Total pore volume, V_p (cm^3/g)	Concentration of functional groups (mmol/g)				
				Carboxyl	Phenolic	Lactone	Total acidic	Basic
RDPP	0.027	0.114	0.255	0.048	0.865	0.274	1.187	2.067
DPAC	316.9	3.204	1.167	0.752	0.694	0.192	1.638	1.602

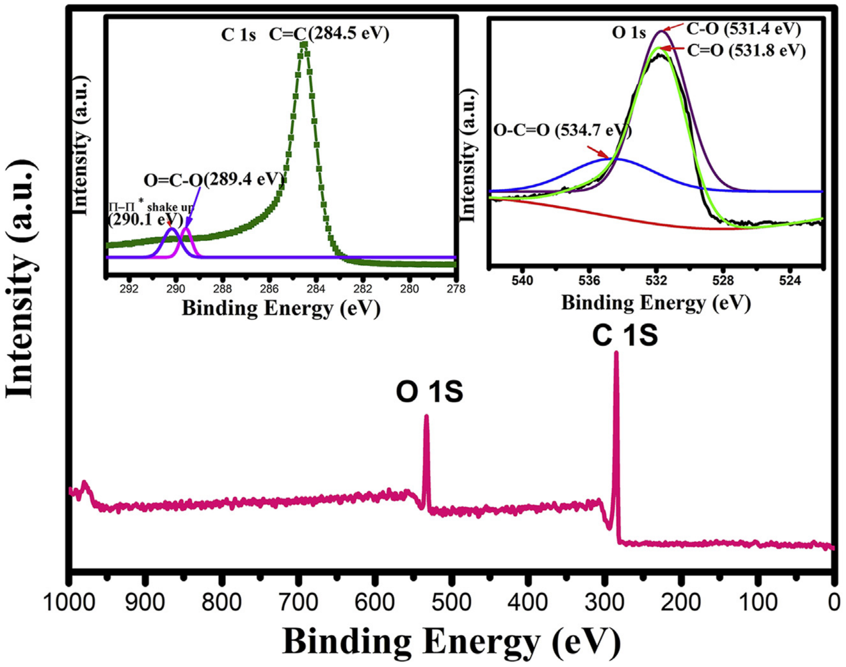

FIG. 1. XPS spectra of pure DPAC sample.

the interactions between the functional groups of the adsorbent DPAC and adsorbate Pb(II) ions. Also the sharp peak felt at $2\theta = 26.5^\circ$ for the spent DPAC indicated the successful binding of the lead metal on DPAC (45).

FTIR spectra of the fresh and Pb(II) adsorbed DPAC samples is shown in Fig. 2B. These absorption spectra display almost the same shape with considerable amount of shifts in their peaks due to Pb(II) adsorption. Significant difference in the spectra for the −OH group presence and absence was seen around 3411 cm^{-1}. The band was quiet wide for fresh DPAC representing the hydrogen bonding between the −OH group (46). The mere disappearance of this stretch for Pb(II) loaded DPAC indicated the interaction between −OH group and Pb(II) ions (38). The −C═O band at 1769 cm^{-1} (carboxyl) and 1059 cm^{-1} (carbonyl) were moved to 1761 cm^{-1} and 1047 cm^{-1} with reduced intensity. In similar fashion, the −C—H band at 1287 cm^{-1} (alkyl halide) and 908 cm^{-1} (aromatics) were relocated to 1279 cm^{-1} and 893 cm^{-1}. These red shifts of the bands with reduced intensities are due to the successful adhesion of metal ions on the DPAC surface (47). In addition, formation of new peak at 516 cm^{-1} can be assigned to the stretching vibration of Pb—O bond, indicating the adsorption of Pb(II) to DPAC surface (48). FTIR studies confirmed the successful binding of Pb(II) ions on DPAC and the functional groups −COO, −CO and −CH were actively involved in the Pb(II) adsorption.

SEM/EDX micro-images of fresh and spent DPAC samples are presented in Fig. 3. SEM studies of both forms of the adsorbents were performed at the same resolution for comparison analysis. As seen in Fig. 3A and B, the SEM micrographs of DPAC clearly illustrated differences in the surface morphology of the DPAC pristine surface and their lead ions loaded surface. The pure surface of DPAC exhibited lamellar and spongy nature with high porosity and significant roughness. The roughness in the surface is due to the existence of various carbon based functional groups present in DPAC. These organizations promote easy diffusion of metal ions to the adsorbent active sites. After adsorption of lead, the surface morphology was changed to much less porous and decreased roughness with well interconnected fibrillary network. EDX spectra for the fresh and Pb(II) loaded DPAC samples are presented in

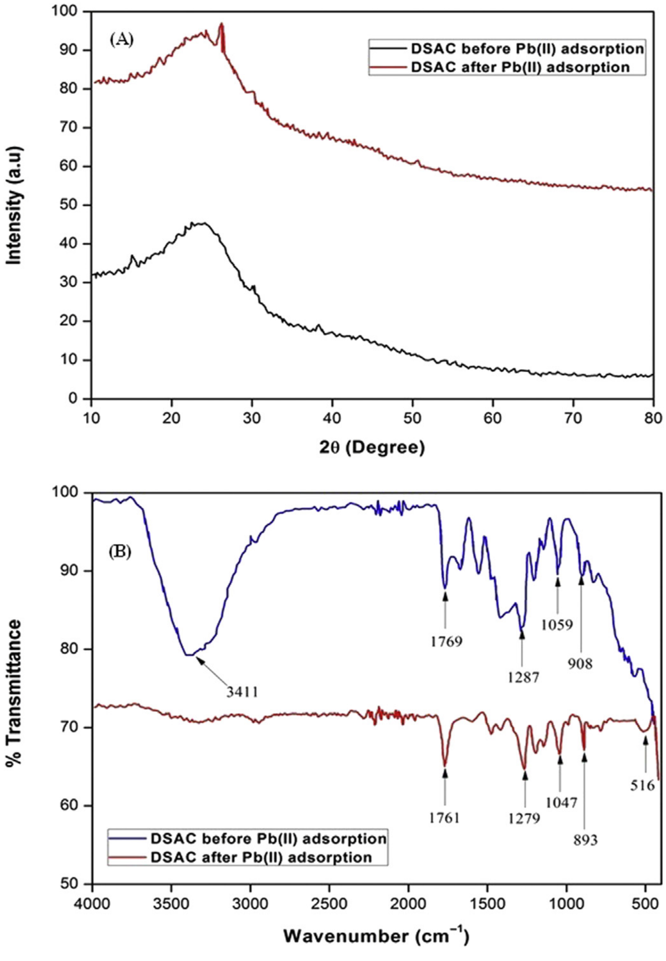

FIG. 2. XRD and FTIR spectra of fresh and expended DPAC surface.

Fig. 3C and D. On comparison, it can be seen that the spectra for spent adsorbent has distinct peaks pertaining to lead metal. Also, the reduced intensity of oxygen in Fig. 3D indicates the interactions of lead and oxygen ions owing to surface adsorption. SEM and EDX results confirmed the Pb(II) ions adhesion on DPAC surface.

Effect of adsorbent dosage and pH Impact of DPAC loading on Pb(II) removal is illustrated in Fig. 4A. Increase in DPAC dosage from 0.5 to 4 g/L improved Pb(II) removal efficiency from 76.8% to 92.6%. Increase in active sites availability for lead ions adsorption with the increase in DPAC dosage produced better lead removal efficiency (24). In contrast, Pb(II) adsorption ability of DPAC got reduced from 136.45 mg/g to 90.16 mg/g with rise in adsorbent dosage. Competition of the Pb(II) ions for adsorption sites (at low adsorbent dosage) and insufficiency of metal ions in liquid phase (at high adsorbent dosage) resulted in the decreased adsorption strength with incremental DPAC dosage. It was also clear that the Pb(II) separation efficiency showed a sharp increase when the DPAC concentration was varied from 0.5 to 2 g/L and reached a plateau nature for further increase of DPAC load. This indicated that 2 g/L of DPAC concentration was an optimal dosage for effective Pb(II) removal for the prescribed experimental conditions.

Fig. 4B explains the results of feed solution pH variation on Pb(II) uptake capacity of DPAC. It was clearly seen that lead adsorption ability enhanced with the increase in feed solution pH from 2 to 6. At low pH, high positive charge density inhibited the adhesion of Pb^{2+} ions on DPAC binding sites. With increase in pH, deprotonation effects caused a rise in negative charge density on DPAC adsorbent promoting the binding of Pb(II) ions. For pH > 6, the adsorption capacity declined due to metal hydroxide formation which precipitates out of the solution making further adsorption studies insignificant (30).

Effect of contact time and initial feed concentration Fig. 4C highlights the influence of contact time and feed solution concentration on DPAC performance for lead ions separation. It was understood that rise in feed concentration results in better uptake ability of Pb(II) on the surface of DPAC. High initial concentration of feed solution produced higher concentration gradient resulting in enhanced driving force for the adsorption process (24). However, the Pb(II) removal efficiency got reduced as 99.4%, 98.1%, 95.6% and 91.4% when the feed concentration was increased as 5, 10, 25 and 50 mg/L. Availability of sufficient binding sites at low feed concentration resulted in high Pb(II) removal efficiency. At high feed concentration, the binding sites were quickly saturated leaving most of the adsorbate in liquid phase itself, causing decreased Pb(II) removal efficiency (28). For contact time, Pb(II) adsorption ability of DPAC showed a sharp increase in initial 30 min and no significant change was observed subsequently after that for all feed concentrations.

Effect of temperature and adsorption thermodynamics Table 3 presents the adsorption capacity of DPAC for changes in the operating temperature from 30°C to 60°C. Results showed that the Pb(II) uptake capacity of DPAC diminished with rise in temperature until 60°C. Studies confirmed the exothermic nature of the lead adsorption on DPAC. Increase in temperature caused the Pb(II) molecules to easily migrate from solid phase to bulk phase resulting in low uptake capacities for DPAC (49). Also, the associated electrostatic interactions involved with Pb(II) binding with DPAC might be weakened which also lead to reduced Pb(II) uptake capacity. Adsorption thermodynamic parameters namely change in Gibbs free energy (ΔG^o), enthalpy (ΔH^o) and entropy (ΔS^o) were obtained by the following equations (50).

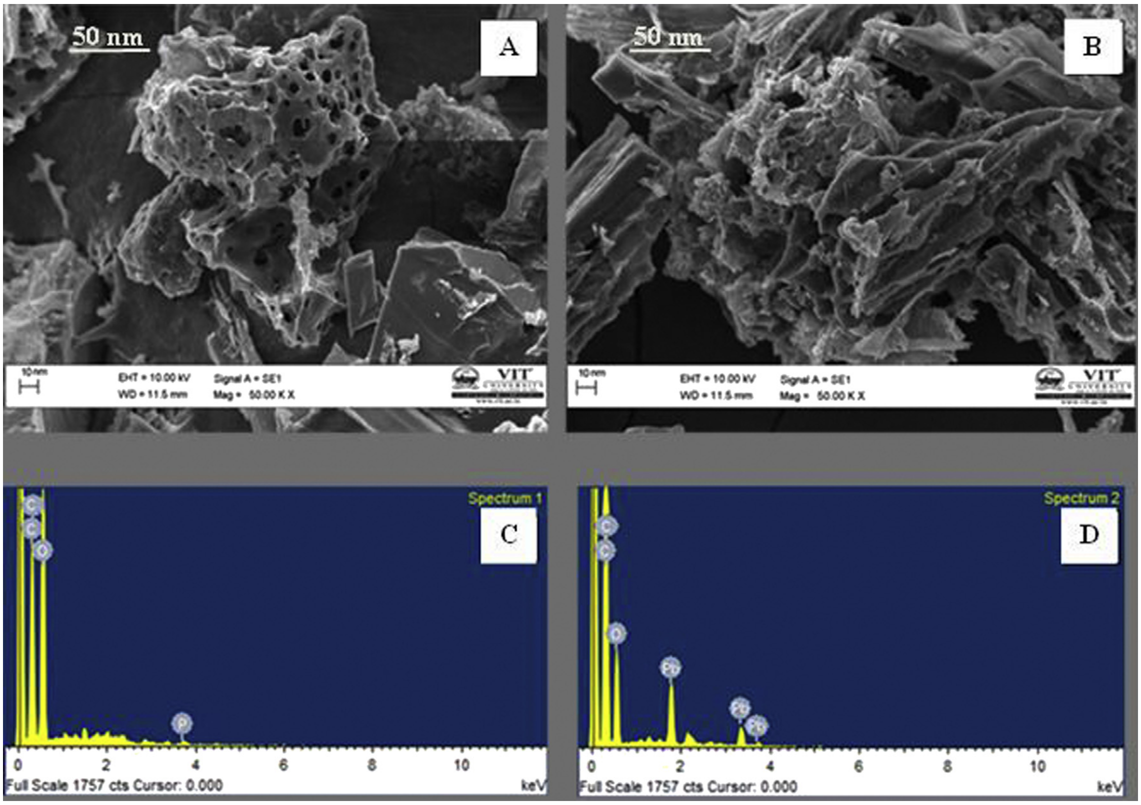

FIG. 3. SEM and EDX micrographs of fresh and spent DPAC surface.

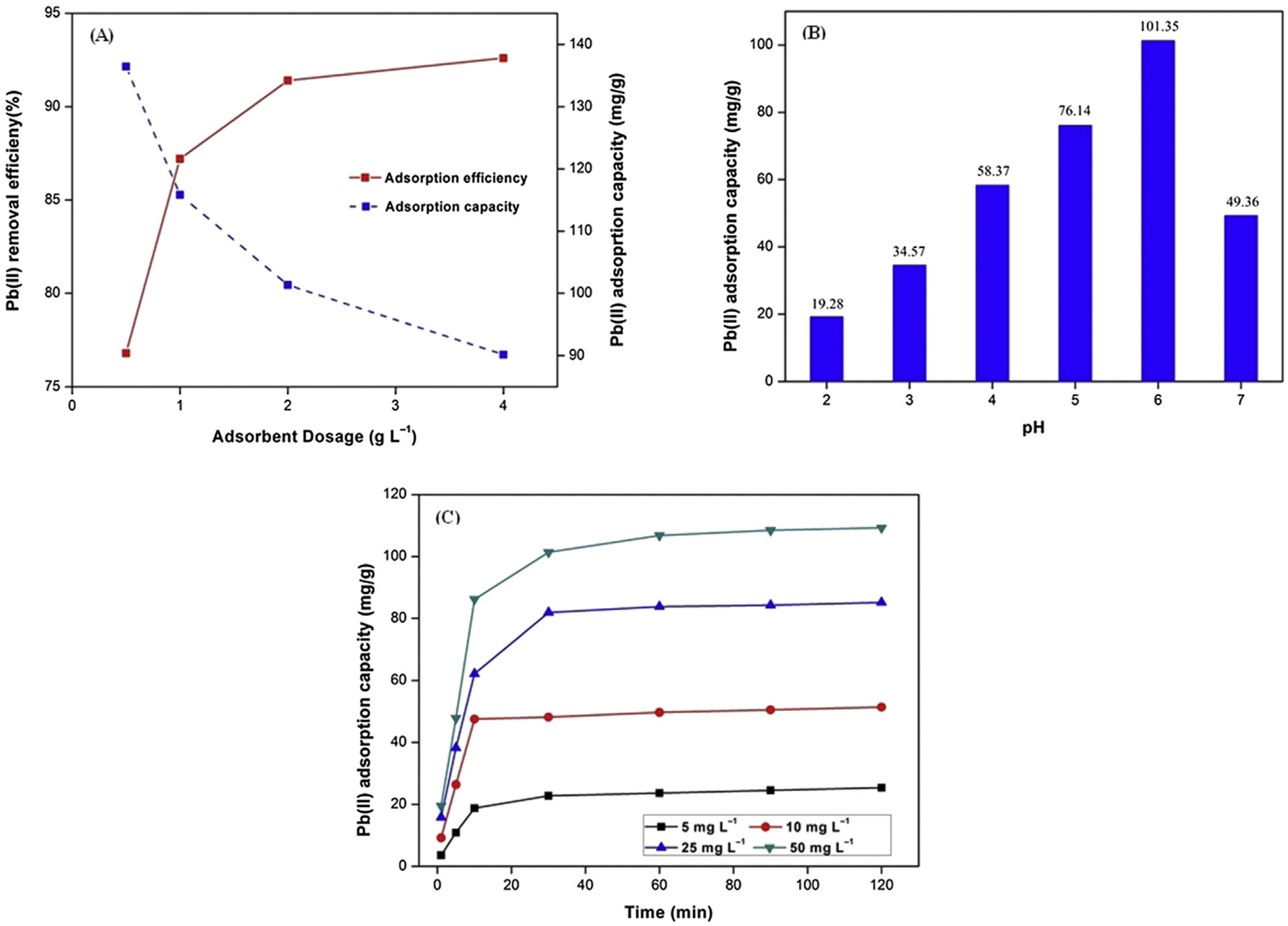

FIG. 4. Influence of adsorption parameters on DPAC performance.

$$\Delta G^{o} = -RT\ln\left(\frac{q_e}{C_e}\right) \tag{10}$$

$$\ln\left(\frac{q_e}{C_e}\right) = \frac{\Delta S^{o}}{R} - \frac{\Delta H^{o}}{RT} \tag{11}$$

ΔH^{o} and ΔS^{o} were evaluated graphically through a plot between ln (q_e/C_e) and $(1/T)$. Table 3 contains the calculated values of the thermodynamics parameters. Negative values of ΔG^{o} confirmed the thermodynamic favor and spontaneity of the adsorption. Lowered negativity of ΔG^{o} with rise in temperature showed the adsorption was more of physical phenomenon (50). Calculated ΔH^{o} being negative revealed the exothermic nature of the adsorption. Decreased randomness at the solid–liquid interface was inferred through the negativity of ΔS^{o} (29).

Adsorption isotherm studies Experiments were performed using adsorbent loading of 1 g/L by varying the initial feed concentrations as 5, 10, 25 and 50 mg/L. Outcomes of the adsorption isotherm analysis are presented in Fig. 5A–C and Table 4. According to Langmuir model, theoretical maximum adsorption capacity (q_{max}) for lead ions uptake by DPAC was computed as 128.21 mg/g at 30°C. Separation factor (R_L) was computed to vary from 0.014 to 0.126 (<1) for Pb(II) adsorption on DPAC surface, which indicated favorable and spontaneous adsorption (51). Parameters for Freundlich constant and exponent were calculated as 4.17 $\text{mg}^{1-1/n}$ $\text{L}^{1/n}$ g^{-1} and 0.35. Temkin isotherm factors were obtained as 17.16 L/mg and 100.55 J g mol^{-1} mg^{-1}. Comparing the determination coefficient (R^2) values for all the studied models, it was concluded that DPAC equilibrium adsorption behavior was according to Langmuir isotherm.

TABLE 3. Temperature studies of Pb(II) adsorption on DPAC.

Temperature (K)	q_e (mg/g)	ΔG^{o} (KJ/mol)	ΔH^{o} (KJ/mol)	ΔS^{o} (KJ/mol)
303	101.35	−7.96	−55.44	−0.16
313	88.49	−6.76		
323	63.72	−5.08		
333	44.23	−3.29		

Adsorption kinetic studies Adsorption dynamics of Pb(II) ions on the prepared DPAC is a key factor for the design projection of DPAC application in column studies. Adsorption tests for kinetics analysis were performed in the time range of 1–120 min. Results for adsorption dynamics are presented in Fig. 5D–F and Table 5. To compare the experimental data with various kinetic models, plots of ln $(q_e - q_t)$ versus t, (t/q_t) versus t and q_e versus $\ln(t)$ were made for pseudo-first order, pseudo-second order and Elovich model respectively. Experimental and kinetic model based theoretical values of the equilibrium adsorption capacity q_e are given in Table 5. From the determination coefficient (R^2) and the closeness of $q_{e,cal}$ with q_e, it was concluded that lead ions adsorption dynamics on DPAC followed pseudo-second order kinetics. Adherence to pseudo-second order kinetics signified the

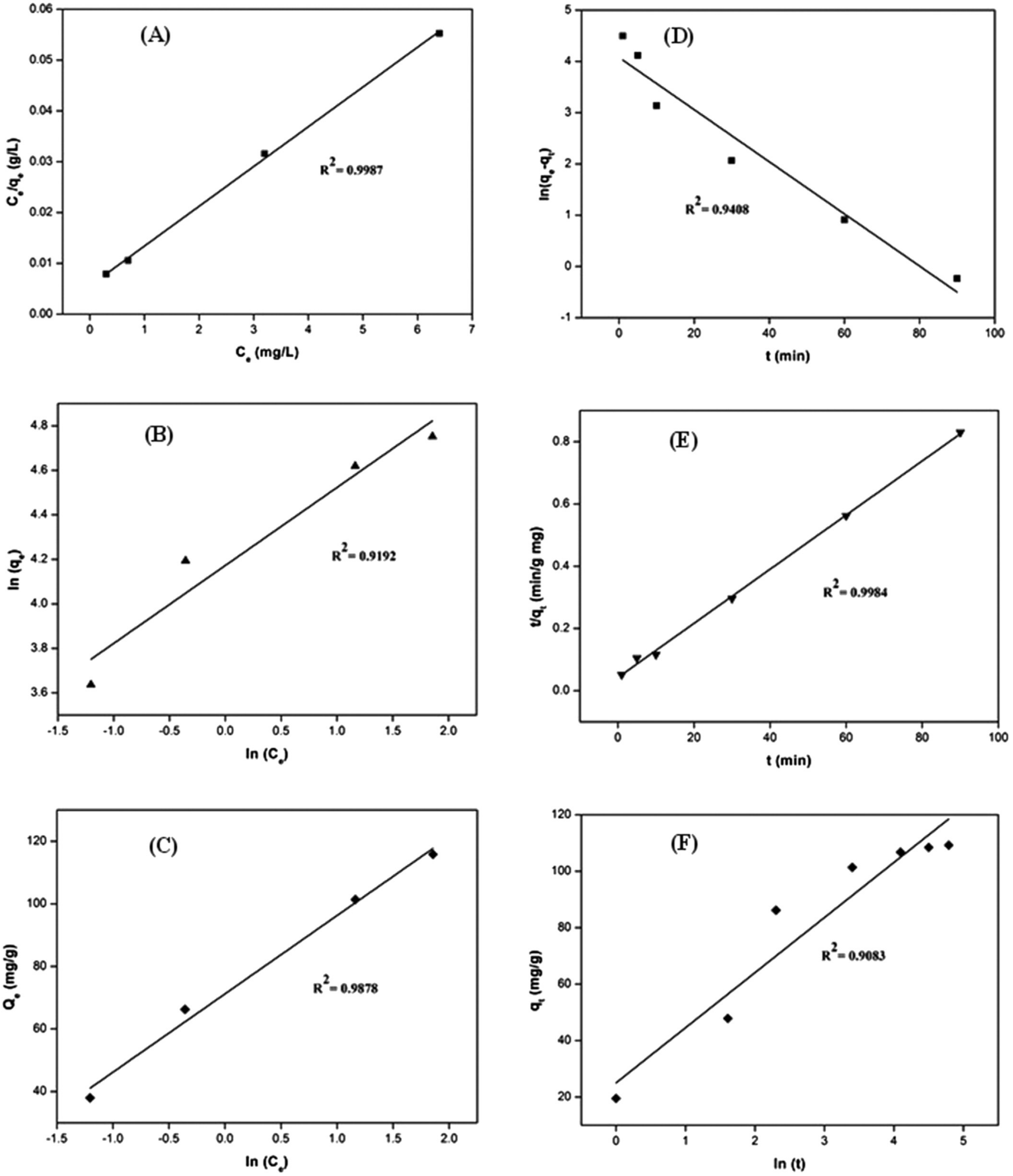

FIG. 5. Isotherm and kinetic studies for Pb(II) adsorption on DPAC surface. (A) Langmuir Isotherm, (B) Freundlich isotherm, (C) Temkin isotherm, (D) pseudo-first order kinetics, (E) pseudo-second order kinetics and (F) Elovich.

TABLE 4. Adsorption isotherm parameters at 30°C.

Langmuir Isotherm			Freundlich Isotherm			Temkin Isotherm		
q_{max} (mg/g)	K_L (L/mg)	R^2	K_f($mg^{1-1/n}$ $L^{1/n}$/g)	1/n	R^2	K_T(L/mg)	b (J g/mol mg)	R^2
128.21	1.39	0.9987	64.87	0.35	0.9192	17.16	100.55	0.9878

TABLE 5. Summary of kinetic models parameters for lead ions uptake by DPAC.

Exp. data	Pseudo-first order			Pseudo-second order			Elovich			
$q_{e,exp}$ (mg/g)	$q_{e,cal}$ (mg/g)	k_1 (1/min)	R^2	$q_{e,cal}$ (mg/g)	k_2 (g/mg min)	R^2	$q_{e,cal}$ (mg/g)	α_E (mg/g min)	β_E (g/mg)	R^2
109.24	58.96	0.0509	0.9408	114.94	0.0018	0.9984	118.53	70.3174	0.0512	0.9083

chemical interactions of Pb(II) ions with DPAC surface involved electron transfers. The initial phase composed of rapid chemisorption of the Pb(II) ions on DPAC followed with the second slow phase of physisorption to reach the equilibrium concentration (52). The same was evident from Fig. 4C where it can be observed that 95% of adsorption capacity was achieved in the first 30 min followed with the sluggish rate of equilibrium capacity attainment in the next 90 min. Plausible mechanism for the Pb^{2+} ion adsorption on the DPAC surface could be explained by electrostatic attraction and ion exchange principle according to equations given below (29):

$$2\ AC - COO^- + Pb^{2+} \leftrightarrow (AC - CO)_2Pb \tag{12}$$

$$2\ AC - COH + Pb^{2+} \leftrightarrow (AC - CO)_2Pb + 2H^+ \tag{13}$$

$$AC - COH_2^{2+} + Pb^{2+} \leftrightarrow AC - COPb^{2+} + 2H^+ \tag{14}$$

where AC refers to the surface carbon chain of DPAC. The release of the H^+ ions according to the principle described was inferable from the increased acidity of the supernatant with increase in the concentration of the Pb(II) feed solution.

Reusability studies Adsorbent reusability is an economically desirable step for extended use of the adsorbent, decreasing the operational cost of the separation process considerably. Also, the reusability studies examines the desorption ability of the adsorbent and the desorbed metal ions may find their reuse in the main/related processes. The spent DPAC samples were regenerated using water, NaOH and HCl as desorbing mediums and subsequently used back in fresh batch run to test their Pb(II) removal efficiencies. The obtained Pb(II) removal efficiency for five recycle runs is plotted in Fig. 6. As inferred from Fig. 6, HCl was quite effective in regenerating the spent DPAC adsorbent as compared with NaOH and water. Regeneration success of HCl is ascribed to the substitution of Pb^{2+} ions by H^+ ions on the DPAC surface. The adsorption sites of DPAC were fully protonated and the recycled DPAC adsorbent was having good Pb(II) adsorption efficiency in the subsequent cycles. It was seen that up to four regeneration cycles, Pb(II) removal efficiency was almost constant with a marginal reduction of about 10% in the removal efficiency (from 89.9% for first run to 80.2% for the fourth run) for HCl regeneration. For water and NaOH regeneration, Pb(II) removal efficiencies of the regenerated DPAC was lowered by more than 10% in the second and third recycle runs respectively. Thus, the results showed that an efficient reusability of prepared DPAC adsorbent was achieved through HCl for a maximum of four cycles under prescribed conditions.

Comparison of carbon from various precursors Table 6 presents a comparison of divalent lead ions adsorption abilities of the synthesized DPAC with activated carbon derived through various carbon precursors. Comparison shows the high Pb(II) uptake strength of DPAC, indicating the potential use of DPAC to remove divalent lead ions from aqueous streams. Application of DPAC for the complete removal of toxic Pb^{2+} ions (~92%) from its aqueous solution with a good degree of regeneration ability makes the DPAC product highly reliable. The on-par/better adsorption capacity of the DPAC for Pb(II) as compared to several other recently reported adsorbents highlights the robustness of the low cost date pits derived activated carbon.

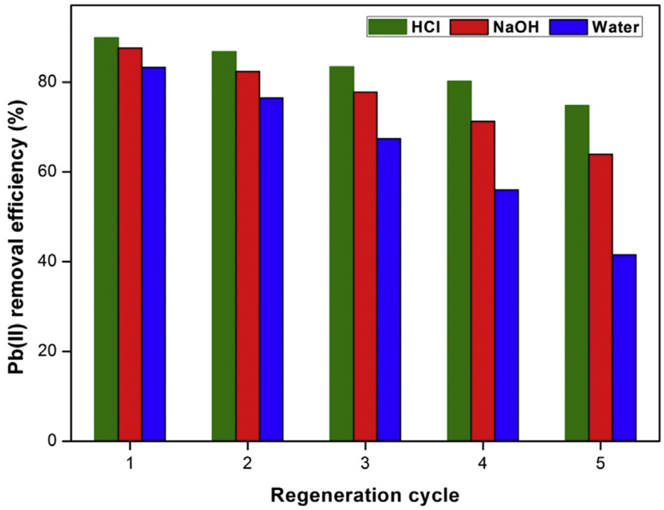

FIG. 6. Reusability studies of spent DSAC using various mediums.

TABLE 6. Pb(II) adsorption capacity of activated carbon derived from different precursors.

Carbon Precursor	Adsorption conditions				Q_{max} (mg/g)	Reference
	pH	T (°C)	Dosage (g/L)	C_i (mg/L)		
Date pit	6	30	2	50	101.35	This study
POME sludge	5.5	30	4	350	62.19	53
Papaya peel	5	–	5	200	38.31	24
Almond shells	5	30	0.5	25	4.5	54
Dindé stones	5	30	0.5	25	7.2	54
Guava seeds	5	30	0.5	25	11.9	54
Bagasse	4	35	1–5	50	52.5	25
Cow bone	4	25	2	100	32.10	30
Van apple pulp	5	25	2.5	40	15.96	4
Coconut shell	3.2–3.6	25	2.0	20–260	40.12	55
Tamarind wood	5.68	30	2	10–50	43.85	56

Conclusions Phosphoric acid based activated carbon prepared from date pits (DPAC) were applied for divalent lead ions separation from its aqueous solution. Studies showed that DPAC is as cheap, abundant, efficient and easy processed adsorbent for efficient removal of Pb(II) from wastewater streams. DPAC was highly porous, amorphous and composed of equal number of acidic and basic functional groups. The synthesized DPAC recorded a Pb(II) uptake capacity superior than activated carbon of commercial type and activated carbon prepared from other lingo-cellulosic materials. Adsorption dependency on various batch process parameters was studied. Adsorption capacity of DPAC improved with incremental pH in acid region as well as with rise in initial feed concentration. Contact time, temperature and adsorbent dosage were analyzed for their optimum values of 30 min, 30°C and 2 g/L. Prepared DPAC possessed an experimental maximum of 101.35 mg/g as Pb(II) uptake capacity for optimal values of adsorption variables. Pb(II) binding on DPAC was concluded as a spontaneous exothermic process from the negativity of calculated Gibbs free energy change and adsorption enthalpy. Equilibrium studies specified the suitability of Langmuir isotherm with a theoretical adsorption capacity of 128.21 mg/g for DPAC under studied conditions. Adsorption kinetic analysis confirmed that the Pb(II) binding to DPAC surface followed pseudo-second order model. Reusability studies proved the economic advantage of expending the regenerated DPAC through HCl for a maximum of four times with a 10% decrease in Pb(II) removal efficiency. Application of the DPAC for other metal pollutants removal from their aqueous streams could be done as a future study. Also a techno-economic study for the industrial application of the prepared DPAC, including the application of DPAC for real time industrial lead effluent treatment, could also be performed as an extension of the current work. Thus the prepared activated carbon from the date pits is very assuring for divalent lead ions removal from wastewater streams.

ACKNOWLEDGMENT

Authors thank the SEM/EDX facility of VIT University for the analysis of the carbon samples.

References

1. **Iwahori, K., Watanabe, J. I., Tani, Y., Seyama, H., and Miyata, N.:** Removal of heavy metal cations by biogenic magnetite nanoparticles produced in Fe (III)-reducing microbial enrichment cultures, J. Biosci. Bioeng., **117**, 333–335 (2014).
2. **Suh, J. H., Yun, J. W., Kim, D. S., and Song, S. K.:** A comparative study on Pb^{2+} accumulation between *Saccharomyces cerevisiae* and *Aureobasidium pullulans* by SEM (scanning electron microscopy) and EDX (energy dispersive X-ray) analyses, J. Biosci. Bioeng., **87**, 112–115 (1999).
3. **Örnek, A., Özacar, M., and Şengil, İ. A.:** Adsorption of lead onto formaldehyde or sulphuric acid treated acorn waste: equilibrium and kinetic studies, Biochem. Eng. J., **37**, 192–200 (2007).
4. **Depci, T., Kul, A. R., and Önal, Y.:** Competitive adsorption of lead and zinc from aqueous solution on activated carbon prepared from Van apple pulp: study in single–and multi–solute systems, Chem. Eng. J., **200**, 224–236 (2012).
5. **Li, K. and Wang, X.:** Adsorptive removal of Pb (II) by activated carbon prepared from *Spartina alterniflora*: equilibrium, kinetics and thermodynamics, Bioresour. Technol., **100**, 2810–2815 (2009).
6. **Goel, J., Kadirvelu, K., Rajagopal, C., and Garg, V. K.:** Removal of lead (II) by adsorption using treated granular activated carbon: batch and column studies, J. Hazard Mater., **125**, 211–220 (2005).
7. **Teoh, Y. P., Khan, M. A., and Choong, T. S.:** Kinetic and isotherm studies for lead adsorption from aqueous phase on carbon coated monolith, Chem. Eng. J., **217**, 248–255 (2013).
8. **World Health Organization:** Guidelines for drinking-water quality, WHO Chronicle, **38**, 104–108 (2011).
9. **Arabi, M., Ghaedi, M., and Ostovan, A.:** Development of a lower toxic approach based on green synthesis of water-compatible molecularly imprinted nanoparticles for the extraction of hydrochlorothiazide from human urine, ACS Sustain. Chem. Eng., **5**, 3775–3785 (2017).
10. **Ostovan, A., Ghaedi, M., Arabi, M., Yang, Q., Li, J., and Chen, L.:** Hydrophilic multitemplate molecularly imprinted biopolymers based on a green synthesis strategy for determination of B-family vitamins, ACS Appl. Mater. Inter., **10**, 4140–4150 (2018).
11. **Ostovan, A., Ghaedi, M., and Arabi, M.:** Fabrication of water-compatible superparamagnetic molecularly imprinted biopolymer for clean separation of baclofen from bio-fluid samples: a mild and green approach, Talanta, **179**, 760–768 (2018).
12. **Ostovan, A., Ghaedi, M., Arabi, M., and Asfaram, A.:** Hollow porous molecularly imprinted polymer for highly selective clean-up followed by influential preconcentration of ultra-trace glibenclamide from bio-fluid, J. Chromatogr. A, **1520**, 65–74 (2017).
13. **Arabi, M., Ostovan, A., Ghaedi, M., and Purkait, M. K.:** Novel strategy for synthesis of magnetic dummy molecularly imprinted nanoparticles based on functionalized silica as an efficient sorbent for the determination of acrylamide in potato chips: optimization by experimental design methodology, Talanta, **154**, 526–532 (2016).
14. **Arabi, M., Ghaedi, M., and Ostovan, A.:** Development of dummy molecularly imprinted based on functionalized silica nanoparticles for determination of acrylamide in processed food by matrix solid phase dispersion, Food Chem., **210**, 78–84 (2016).
15. **Arabi, M., Ghaedi, M., and Ostovan, A.:** Water compatible molecularly imprinted nanoparticles as a restricted access material for extraction of hippuric acid, a biological indicator of toluene exposure, from human urine, Microchim. Acta, **184**, 879–887 (2017).
16. **Arabi, M., Ghaedi, M., and Ostovan, A.:** Synthesis and application of in-situ molecularly imprinted silica monolithic in pipette-tip solid-phase microextraction for the separation and determination of gallic acid in orange juice samples, J. Chromatogr. B, **1048**, 102–110 (2017).
17. **Baral, S. S., Das, S. N., and Rath, P.:** Hexavalent chromium removal from aqueous solution by adsorption on treated sawdust, Biochem. Eng. J., **31**, 216–222 (2006).
18. **Foo, K. Y. and Hameed, B. H.:** An overview of dye removal via activated carbon adsorption process, Desalin. Water Treat., **19**, 255–274 (2010).
19. **Wong, S., Ngadi, N., Inuwa, I. M., and Hassan, O.:** Recent advances in applications of activated carbon from biowaste for wastewater treatment: a short review, J. Clean. Prod., **175**, 361–375 (2018).
20. **Marsh, H. and Reinoso, F. R.:** Activated carbon. Elsevier Science, Amsterdam (2006).
21. **Gupta, V. K., Carrott, P. J. M., Singh, R., Chaudhary, M., and Kushwaha, S.:** Cellulose: a review as natural, modified and activated carbon adsorbent, Bioresour. Technol., **216**, 1066–1076 (2016).
22. **Altenor, S., Carene, B., Emmanuel, E., Lambert, J., Ehrhardt, J., and Gaspard, S.:** Adsorption studies of methylene blue and phenol onto vetiver roots activated carbon prepared by chemical activation, J. Hazard. Mater., **165**, 1029–1039 (2009).
23. **Elizalde-González, M. P. and Hernández-Montoya, V.:** Characterization of mango pit as raw material in the preparation of activated carbon for wastewater treatment, Biochem. Eng. J., **36**, 230–238 (2007).
24. **Abbaszadeh, S., Alwi, S. R. W., Webb, C., Ghasemi, N., and Muhamad, I. I.:** Treatment of lead–contaminated water using activated carbon adsorbent from locally available papaya peel biowaste, J. Clean. Prod., **118**, 210–222 (2016).
25. **Tao, H. C., Zhang, H. R., Li, J. B., and Ding, W. Y.:** Biomass based activated carbon obtained from sludge and sugarcane bagasse for removing lead ion from wastewater, Bioresour. Technol., **192**, 611–617 (2015).
26. **Adibmehr, M. and Faghihian, H.:** Magnetization and functionalization of activated carbon prepared by oak shell biowaste for removal of Pb^{2+} from aqueous solutions, Chem. Eng. Commun., **205**, 519–532 (2018).
27. **Momčilović, M., Purenović, M., Bojić, A., Zarubica, A., and Ranđelović, M.:** Removal of lead (II) ions from aqueous solutions by adsorption onto pine cone activated carbon, Desalination, **276**, 53–59 (2011).
28. **Imamoglu, M. and Tekir, O.:** Removal of copper (II) and lead (II) ions from aqueous solutions by adsorption on activated carbon from a new precursor hazelnut husks, Desalination, **228**, 108–113 (2008).
29. **Sekar, M., Sakthi, V., and Rengaraj, V. S.:** Kinetics and equilibrium adsorption study of lead (II) onto activated carbon prepared from coconut shell, J. Colloid Interface Sci., **279**, 307–313 (2004).
30. **Cechinel, M. A. P. and de Souza, A. A. U.:** Study of lead (II) adsorption onto activated carbon originating from cow bone, J. Clean. Prod., **65**, 342–349 (2014).
31. **Liu, Q. S., Zheng, T., Wang, P., and Guo, L.:** Preparation and characterization of activated carbon from bamboo by microwave-induced phosphoric acid activation, Ind. Crop. Prod., **31**, 233–238 (2010).
32. **Dias, J. M., Alvim-Ferraz, M. C., Almeida, M. F., Rivera-Utrill, J., and Sánchez-Polo, M.:** Waste materials for activated carbon preparation and its use in aqueous–phase treatment: a review, J. Environ. Manag., **85**, 833–846 (2007).
33. **Ogungbenro, A. E., Quang, D. V., Al-Ali, K., and Abu-Zahra, M. R.:** Activated carbon from date seeds for CO_2 capture application, Energ. Procedia, **114**, 2313–2321 (2017).
34. **Ahmed, M. J. and Theydan, S. K.:** Physical and chemical characteristics of activated carbon prepared by pyrolysis of chemically treated date stones and its ability to adsorb organics, Powder Technol., **229**, 237–245 (2012).
35. **Bouchelta, C., Medjram, M. S., Bertrand, O., and Bellat, J. P.:** Preparation and characterization of activated carbon from date stones by physical activation with steam, J. Anal. Appl. Pyrol., **82**, 70–77 (2008).
36. **Salman, J. M., Njoku, V. O., and Hameed, B. H.:** Bentazon and carbofuran adsorption onto date seed activated carbon: kinetics and equilibrium, Chem. Eng. J., **173**, 361–368 (2011).

37. **Islam, M. A., Tan, I. A. W., Benhouria, A., Asif, M., and Hameed, B. H.:** Mesoporous and adsorptive properties of palm date seed activated carbon prepared via sequential hydrothermal carbonization and sodium hydroxide activation, Chem. Eng. J., **270**, 187–195 (2015).
38. **Yakubu, M. K., Gumel, M. S., and Abdullahi, A. M.:** Use of activated carbon from date seeds to treat textile and tannery effluents, Afr. J. Sci. Technol., **9**, 39–49 (2008).
39. **Bunluesin, S., Kruatrachue, M., Pokethitiyook, P., Upatham, S., and Lanza, G. R.:** Batch and continuous packed column studies of cadmium biosorption by *Hydrilla verticillata* biomass, J. Biosci. Bioeng., **103**, 509–513 (2007).
40. **Oyetibo, G. O., Miyauchi, K., Suzuki, H., Ishikawa, S., and Endo, G.:** Extracellular mercury sequestration by exopolymeric substances produced by *Yarrowia* spp.: thermodynamics, equilibria, and kinetics studies, J. Biosci. Bioeng., **122**, 701–707 (2016).
41. **Omri, A., Wali, A., and Benzina, M.:** Adsorption of bentazon on activated carbon prepared from Lawsonia inermis wood: equilibrium, kinetic and thermodynamic studies, Arab. J. Chem., **9**, S1729–S1739 (2016).
42. **Gupta, V. K., Kumar, R., Nayak, A., Saleh, T. A., and Barakat, M. A.:** Adsorptive removal of dyes from aqueous solution onto carbon nanotubes: a review, Adv. Colloid Interface, **193**, 24–34 (2013).
43. **Stafiej, A. and Pyrzynska, K.:** Adsorption of heavy metal ions with carbon nanotubes, Sep. Purif. Technol., **58**, 49–52 (2007).
44. **Dawodu, F. A. and Akpomie, K. G.:** Simultaneous adsorption of Ni (II) and Mn (II) ions from aqueous solution unto a Nigerian kaolinite clay, J. Mat. Res. Technol., **3**, 129–141 (2014).
45. **Chen, P. Y., Qi, J., Klug, M. T., Dang, X., Hammond, P. T., and Belcher, A. M.:** Environmentally responsible fabrication of efficient perovskite solar cells from recycled car batteries, Energy Environ. Sci., **7**, 3659–3665 (2014).
46. **Escudero, C., Fiol, N., Villaescusa, I., and Bollinger, J. C.:** Arsenic removal by a waste metal hydroxide entrapped into calcium alginate beads, J. Hazard. Mater., **164**, 533–554 (2009).
47. **Lalhruaitluanga, H., Jayaram, K., Prasad, M. N. V., and Kumar, K. K.:** Lead (II) adsorption from aqueous solutions by raw and activated charcoals of *Melocanna baccifera* Roxburgh (bamboo)—a comparative study, J. Hazard. Mater., **175**, 311–318 (2010).
48. **Bosca, M., Pop, L., Borodi, G., Pascuta, P., and Culea, E.:** XRD and FTIR structural investigations of erbium–doped bismuth–lead–silver glasses and glass ceramics, J. Alloy. Comp., **479**, 579–582 (2009).
49. **Gupta, V. K., Gupta, B., Rastogi, A., Agarwal, S., and Nayak, A.:** A comparative investigation on adsorption performances of mesoporous activated carbon prepared from waste rubber tire and activated carbon for a hazardous azo dye—acid Blue 113, J. Hazard. Mater., **186**, 891–901 (2011).
50. **Senthilkumar, R., Vijayaraghavan, K., Thilakavathi, M., Iyer, P. V. R., and Velan, M.:** Application of seaweeds for the removal of lead from aqueous solution, Biochem. Eng. J., **33**, 211–216 (2007).
51. **Foo, K. Y. and Hameed, B. H.:** Insights into the modeling of adsorption isotherm systems, Chem. Eng. J., **156**, 2–10 (2010).
52. **Saeidi, N., Parvini, M., and Niavarani, Z.:** High surface area and mesoporous graphene/activated carbon composite for adsorption of Pb (II) from wastewater, J. Environ. Chem. Eng., **3**, 2697–2706 (2015).
53. **Adebisi, G. A., Chowdhury, Z. Z., and Alaba, P. A.:** Equilibrium, kinetic, and thermodynamic studies of lead ion and zinc ion adsorption from aqueous solution onto activated carbon prepared from palm oil mill effluent, J. Clean. Prod., **148**, 958–968 (2017).
54. **Brudey, T., Largitte, L., Jean-Marius, C., Tant, T., Dumesnil, P. C., and Lodewyckx, P.:** Adsorption of lead by chemically activated carbons from three lignocellulosic precursors, J. Anal. Appl. Pyrol., **120**, 450–463 (2016).
55. **Song, X., Liu, H., Cheng, L., and Qu, Y.:** Surface modification of coconut–based activated carbon by liquid–phase oxidation and its effects on lead ion adsorption, Desalination, **255**, 78–83 (2010).
56. **Acharya, J., Sahu, J. N., Mohanty, C. R., and Meikap, B. C.:** Removal of lead(II) from wastewater by activated carbon developed from Tamarind wood by zinc chloride activation, Chem. Eng. J., **149**, 249–262 (2009).